Energy and electron spectra after grazing-ion–surface collisions

M. S. Gravielle and J. E. Miraglia
Instituto de Astronomía y Física del Espacio (IAFE), Consejo Nacional de Investigaciones Científicas y Técnicas, C.C. 67, Suc. 28, 1428 Buenos Aires, Argentina
and Departamento de Física, FCEN, Universidad de Buenos Aires, Buenos Aires, Argentina
(Received 18 July 2001; published 4 January 2002)

For ions that impinge grazing on solid surfaces, binary collisions with the free-electron gas are investigated by means of a modified specular-reflection (MSR) model. The proposed MSR theory is applied to the calculation of the energy lost by fast protons after colliding with an aluminum surface. We also employ the MSR binary theory to study the energy spectra of the emitted electrons. The contribution coming from atomic inner shells, calculated with the continuum-distorted-wake–eikonal-initial-state approximation, is added to the emission probability from the valence band. The total results obtained with the MSR model are in reasonable agreement with available experimental data for 100 keV protons and large ejection angles of the electron. In contrast instead, the usual specular-reflection binary model shows a prominent structure at low electron energies, which greatly overstimates the experimental spectrum.

DOI: 10.1103/PhysRevA.65.022901 PACS number(s): 34.50.Dy, 34.50.Bw

I. INTRODUCTION

When a fast ion collides grazingly with a metal surface, it loses energy as a consequence of the ionization of electrons bound to surface atoms and of the excitation of conduction electrons of the solid. Two different mechanisms participate in the second process: the excitation of the plasmon field and binary electron excitation. The plasmon excitation involves the collective response of the medium to the moving ion, while the binary excitations take into account single collisions of the projectile with valence electrons, which compose the free-electron gas. We are interested in this latter mechanism, usually called the binary mechanism, which provides an important contribution to the energy loss when the ion moves in the proximity of the surface. Our final goal is to describe the angular and energy distributions of electrons ejected as a result of the ion-surface collision, whose study is the objective of recent experimental works [1,2].

In previous articles [3,4] we evaluated the collisions of the incident ion with individual valence electrons with a binary collisional theory, employing different models to describe the surface induced potential. Mentioned in increasing order of complexity, these approximations were a simple Yukawa-type potential, the parallel dispersion (PD) model [5,6], and the well-known specular-reflection (SR) model [7,8]. While the first potential represents only a spherically symmetric projectile-electron interaction, the other two models are derived from the dielectric theory for semi-infinite media, taking into consideration, albeit approximately, the presence of the surface. However, it has been found that the binary theory fails to describe the energy loss near the surface, even if the more elaborate SR model is used [4]. The failure of the binary results can be attributed to the fact that the component of the transferred momentum perpendicular to the surface is absent completely or on an average way in the PD and SR wake potentials, respectively.

In the present work we introduce a modification in the SR model within the binary collisional formalism, which leads to what we call the modified specular-reflection (MSR) model. This modification is based on the inclusion of the momentum transfer perpendicular to the surface in the wake potential. Energy-loss results obtained with the proposed model are compared with those derived from the usual dielectric formulation [9,10]. The MSR binary model is also applied to calculate the electron emission induced by the projectile. In order to compare the emission probabilities with available experimental spectra [11] we evaluate the inner-shell emission yield. It is calculated by employing the continuum-distorted-wave–eikonal-initial-state (CDW-EIS) approximation to describe the atomic ionization probabilities, taking into consideration the full dependency on the impact parameter [12].

The collision system composed of fast protons impinging on an aluminum surface is here used as a benchmark for the theory. The energies considered correspond to the high-velocity range, i.e., $v_i > v_F$, where v_i is the projectile impact velocity and v_F is the Fermi velocity of the free-electron gas. In this velocity range protons can be considered as bare ions along the whole trajectory [13,14]. As usual, to describe the binary collisions with the conduction electrons we employ a semiclassical formalism, in which the trajectory of the incident ion is classically determined [3]. The free-electron gas is represented with the simple surface jellium approximation, and the *T*-matrix element that describes the electronic transition is evaluated by using the first Born approximation. The work is organized as follows. In Sec. II we introduce the proposed theoretical model. Energy-loss results are presented in Sec. III A, and in Sec. III B differential emission probabilities are investigated, comparing them with available experimental data. Section IV contains our conclusions. Atomic units are used unless otherwise stated.

II. THEORETICAL MODEL

We consider a heavy projectile (P) of charge Z_P impinging on a solid surface with a glancing incidence angle. As a result of the collision an electron (e) with initial momentum $\mathbf{k}_i$, belonging to the valence band of the solid, is excited to a state with momentum $\mathbf{k}_f$. The frame of reference is fixed to the position of the electronic surface, which is placed at a

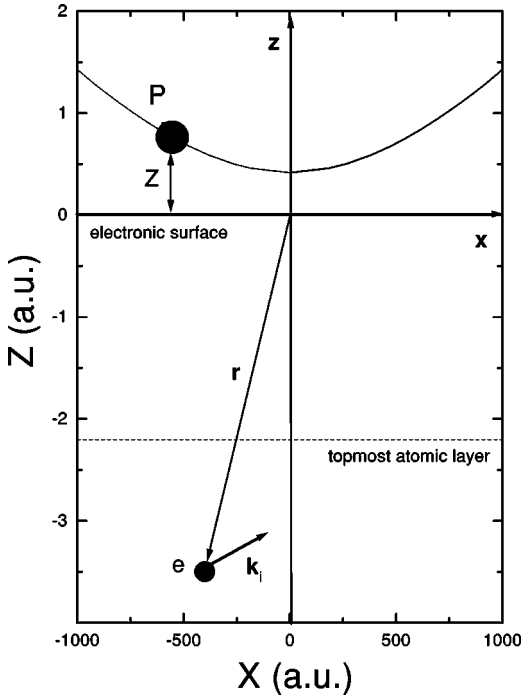

FIG. 1. Schematic picture of the coordinate system.

distance $d/2$ in front of the first atomic layer, d being the interplanar separation. In this frame the classical projectile path is contained in the x-z plane and the surface in the x-y plane (see Fig. 1). Due to the symmetry of our problem, it is convenient to decompose the vectors into a two-dimensional vector parallel to the surface and a component perpendicular to the surface. In this way, the projectile velocity at the time t is written as $\mathbf{v}=(\mathbf{v}_s,v_z)$.

Within the binary collisional formalism the transition probability per unit time reads [3]

$$\frac{dP'}{d\mathbf{k}_i d\mathbf{k}_f}=2\pi\delta(\Delta)|\mathcal{T}(\mathbf{k}_i,\mathbf{k}_f)|^2, \tag{1}$$

where $\mathcal{T}(\mathbf{k}_i,\mathbf{k}_f)$ is the T-matrix element corresponding to the inelastic transition $\mathbf{k}_i\rightarrow\mathbf{k}_f$. The δ function imposes the energy conservation, $\Delta=-E_{if}+\mathbf{v}_s\cdot(\mathbf{k}_f-\mathbf{k}_i)$, and $E_{if}=E_{\mathbf{k}_f}-E_{\mathbf{k}_i}$ is the energy gained by the electron (and lost by the projectile) in the collision. In the first Born approximation, the T-matrix element reads $\mathcal{T}^{\mathrm{B}}(\mathbf{k}_i,\mathbf{k}_f)=\langle\phi^-_{\mathbf{k}_f}|V_{Pe}|\phi^+_{\mathbf{k}_i}\rangle$, where V_{Pe} is the Coulomb P-e interaction shielded by the presence of the other valence electrons, and $\phi^+_{\mathbf{k}_i}$ and $\phi^-_{\mathbf{k}_f}$ are the initial and final electronic states, respectively.

We use the surface jellium model to represent the conduction band of the solid. In this model the electrons are considered independent and confined in the $z<0$ region by a square barrier of depth $V_0=E_F+E_W$, with E_F the Fermi energy and E_W the work function. Within the jellium model the electronic wave functions are written as $\phi^{\pm}_{\mathbf{k}}(\mathbf{r})=(2\pi)^{-1}\exp(i\mathbf{k}_s\cdot\mathbf{r}_s)\varphi^{\pm}_{k_z}(r_z)$, where $\mathbf{r}=(\mathbf{r}_s,r_z)$ is the position vector of the electron, $\mathbf{k}=(\mathbf{k}_s,k_z)$ is the electron momentum inside the solid, and $E_{\mathbf{k}}=k_s^2/2+\epsilon_{k_z}$ is the electron energy. The sign $\pm$ indicates the incoming $(-)$ and outgoing $(+)$ asymptotic conditions, and the eigenfunctions $\varphi^{\pm}_{k_z}$ are defined in the Appendix of Ref. [3]. The T-matrix element $\mathcal{T}^{\mathrm{B}}(\mathbf{k}_i,\mathbf{k}_f)$ can be expressed as an integral in the momentum space:

$$\mathcal{T}^{\mathrm{B}}(\mathbf{k}_i,\mathbf{k}_f)=\frac{1}{(2\pi)^4}\int_{-\infty}^{+\infty}du\,\tilde{V}_{Pe}(u)f(u), \tag{2}$$

where $\tilde{V}_{Pe}(u)$ is the Fourier transform of V_{Pe} evaluated on $(\mathbf{p}_s,u)$, $\mathbf{p}=\mathbf{k}_f-\mathbf{k}_i=(\mathbf{p}_s,p_z)$ is the transferred electron momentum, and $f(u)=\langle\varphi^-_{k_{fz}}|\exp(iur_z)|\varphi^+_{k_{iz}}\rangle$ is the one-dimensional electronic form factor. The function $\tilde{V}_{Pe}$ can be expressed as $\tilde{V}_{Pe}(u)=\tilde{V}_C(u)W_{Pe}(u)$, where $\tilde{V}_C(u)=2(2\pi)^2Z_P/(p_s^2+u^2)$ is the Fourier transform of the Coulomb P-e potential and $W_{Pe}(u)$ is a screening factor, which depends on the approximation used to describe the induced potential.

To derive the proposed model we start from the usual SR approximation [7,8], in which the screening factor reads [4]

$$\begin{aligned}W^{(SR)}_{Pe}(u)&=\left[\frac{\epsilon'_s(u,0)\delta_s^2-p_s-iu\epsilon_s(0)}{p_s[1+\epsilon_s(0)]}\exp(-p_sZ)\right.\\&\left.+\exp(-iuZ)\right]\Theta(Z)+\frac{\delta_s^2}{p_s}\left[\frac{\epsilon'_s(u,Z)+\epsilon'_s(u,-Z)}{2}\right.\\&\left.+\frac{\epsilon_s(Z)}{[1+\epsilon_s(0)]}\left(\frac{1}{p_s+iu}-\epsilon'_s(u,0)\right)\right]\Theta(-Z),\end{aligned} \tag{3}$$

with $\delta_s^2=p_s^2+u^2$,

$$\epsilon'_s(u,z)=\int_{-\infty}^{0}dz'\exp(-iuz')\epsilon_s(z'-z), \tag{4}$$

and

$$\epsilon_s(z)=\frac{p_s}{\pi}\int_{-\infty}^{+\infty}dq_z\frac{\exp(iq_zz)}{(p_s^2+q_z^2)}\frac{1}{\epsilon(\mathbf{p}_s+q_z\hat{\mathbf{z}},\omega)}, \tag{5}$$

where $\epsilon(\mathbf{q},\omega)$ is the bulk dielectric function evaluated using the momentum $\mathbf{q}=\mathbf{p}_s+q_z\hat{\mathbf{z}}$ and the frequency $\omega=\mathbf{p}\cdot\mathbf{v}_s$. In Eq. (3), Θ denotes the unitary Heaviside function. Since Eq. (5) involves an integral over q_z, the distribution of the transferred momentum perpendicular to the surface, which is determined by $\epsilon(\mathbf{q},\omega)$, is present in an average way in the SR potential. Nevertheless, the knowledge of the specific q_z distribution is essential to describe single-particle collisions. Lack of this information is then the origin of the failure of the usual SR binary theory, as observed in Ref. [4]. Note also that in the SR model the q_z average is linked to the fact that an *infinite* barrier is involved in the calculation of the induced potential, whereas the jellium wave functions employed in the binary formalism correspond to a *finite* barrier.

Deep inside the solid, where plane waves can be used to represent both the electronic states and the bulk response function (with the random-phase approximation), binary momentum conservation states that the momentum lost by the projectile is equal to that gained by the electron, i.e., $\mathbf{q}=\mathbf{p}$ [15]. Accordingly, we introduce the MSR model by singling out in the dielectric function the particular value $q_z = p_z$ that satisfies the momentum conservation. In other words, the MSR model is obtained from Eq. (5) by replacing q_z by p_z in the argument of the bulk response function. Then, the screening factor $W_{Pe}^{(MSR)}(u)$ is derived from Eq. (3) by replacing $\epsilon_s(z)$ by

$$\epsilon_s^{(MSR)}(z) = \frac{p_s}{\pi}\int_{-\infty}^{+\infty} dq_z \frac{\exp(iq_z z)}{(p_s^2+q_z{}^2)}\frac{1}{\epsilon(\mathbf{p},\omega)} = [\epsilon(\mathbf{p},\omega)]^{-1}\exp(-p_s|z|), \tag{6}$$

and it reads

$$W_{Pe}^{(MSR)}(u) = \left[\frac{(1-\epsilon)}{(1+\epsilon)}\exp(-p_s|Z|)+\exp(-iuZ)\right]\Theta(Z) - \frac{1}{\epsilon}\left[\frac{(1-\epsilon)}{(1+\epsilon)}\exp(-p_s|Z|) - \exp(-iuZ)\right]\Theta(-Z), \tag{7}$$

with $\epsilon=\epsilon(\mathbf{p},\omega)$ the bulk dielectric function evaluated using the *total* momentum $\mathbf{p}$. The PD model can be derived from Eq. (7) by neglecting the dispersion perpendicular to the surface, that is, the dependency on p_z in the bulk response function, which leads to $\epsilon \simeq \epsilon(\mathbf{p}_s,\omega)$.

Two macroscopic magnitudes associated with ion-surface collisions are examined in this work: the energy lost by the projectile per unit time, S, defined as

$$S = \int d\mathbf{k}_f \int d\mathbf{k}_i \rho_e \Theta(v_F - k_i)\Theta(k_f - v_F) E_{if} \frac{dP'}{d\mathbf{k}_i d\mathbf{k}_f}, \tag{8}$$

and the differential probability of electron emission, $d^3P/d\mathbf{k}_f$, for the transition to a given final state with momentum $\mathbf{k}_f$, which reads

$$\frac{d^3P}{d\mathbf{k}_f} = 2\int_{Z_0}^{+\infty} dZ \frac{1}{|v_z|}\int d\mathbf{k}_i \rho_e \Theta(v_F - k_i)\frac{dP'}{d\mathbf{k}_i d\mathbf{k}_f}. \tag{9}$$

In both expressions the function $\Theta(v_F-k_i)$ restricts the initial states to those contained inside the Fermi sphere and $\rho_e=2$ takes into account the spin states. In Eq. (8) the function $\Theta(k_f-v_F)$ includes the Pauli exclusion principle, while in Eq. (9) the Z integral represents the integration over the projectile trajectory, with Z_0 being the distance of closest approach to the electronic surface. In the derivation of $d^3P/d\mathbf{k}_f$ the incoming and outgoing projectile paths have been considered equivalent. The trajectory of the incident ion is determined by the projectile-surface interaction, which is here described as the Molière potential [16] plus the dynamical image potential given in Ref. [17]. The z component of the projectile velocity, v_z, is derived from energy conservation in the direction perpendicular to the surface along the classical path.

III. RESULTS

Our study is confined to fast protons grazingly impinging on an Al(111) surface. In the calculations, the bulk dielectric function $\epsilon(\mathbf{q},\omega)$ is evaluated by employing the random-phase approximation (Lindhard's dielectric function) [18] together with Mermin's prescription, which allows us to deal with finite values of the lifetime $1/\gamma$ [19]. The parameters used to describe the aluminum surface are the Fermi energy $E_F=0.414$ a.u. ($v_F=0.91$ a.u.), the interplanar distance $d=4.4$ a.u., the work function $E_W=0.15$ a.u., and the damping coefficient $\gamma=0.037$ a.u. [17].

For the evaluation of S, the five-dimensional integration over the momenta involved in Eq. (8) was resolved with the Monte Carlo numerical technique with a relative error less than 1%. While our previous calculations of the binary energy loss with the SR model involved a huge computational effort [4], as a consequence of the additional numerical integration given by Eq. (5), the computation with the MSR model is much faster, as the screening factor given by Eq. (7) has a closed form. For the differential emission probability, the numerical integration over $\mathbf{k}_i$ in Eq. (9) was done with a relative error of 1%, and the further integration on the projectile trajectory was solved by interpolating approximately 30 pivots. Previous binary results from Ref. [3], which were calculated employing a Yukawa potential to represent the effective P-e interaction, are also shown in Figs. 2–5 below as a reference. In general, central potentials have been extensively used to evaluate total stopping power in solids [20].

A. Energy loss

For 700 keV protons, the energy loss per unit time, S, is plotted as a function of the projectile distance to the jellium edge in Fig. 2. For this particular system, theoretical and experimental results have been reported in Refs. [9] and [21], respectively. Binary values obtained with the MSR model are displayed together with data derived from the full dielectric formalism by using the SR wake potential, i.e., Eqs. (6)–(8) of Ref. [9]. Since the dielectric formulation includes both binary collisions *and* collective modes, without separating their contributions, the dielectric data represent the *total* valence contribution to the energy loss. Inside the solid our dielectric values coincide with those of Juaristi *et al.* [9] obtained using the same approximation (with slightly different parameters), but some differences are found in the vacuum region ($Z>0$). As expected, the MSR binary energy loss does not exceed the total valence contribution; that is, MSR binary results are lower than the dielectric data in the whole Z range. In the bulk, below the atomic surface, the MSR binary values approach one-half of the total valence contribution, in agreement with the equipartition rule [18]. This rule states that the energy lost by the projectile in a solid is

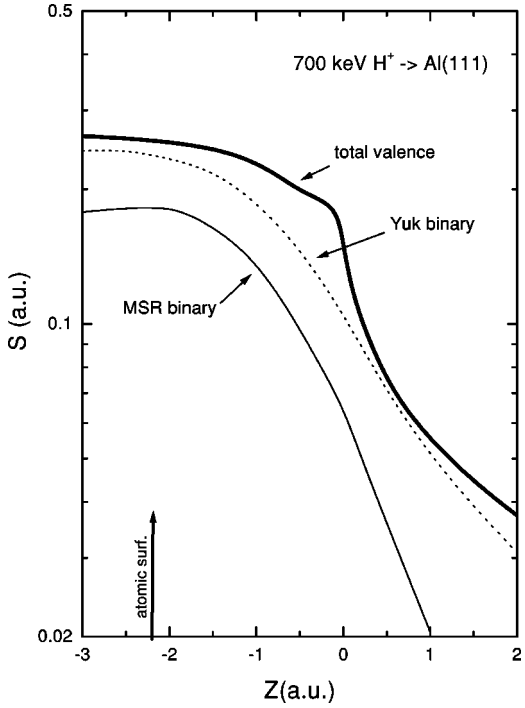

FIG. 2. Energy loss per unit time, S, by collisions with the valence band, as a function of the projectile distance to the electronic surface, Z, for 700 keV protons impinging on an Al(111) surface. Thin solid line, binary collisional contribution calculated with the MSR induced potential [Eq. (7)]; thick solid line, total valence contribution obtained from the dielectric formalism, as explained in the text. The dotted line corresponds to binary collisional results of Ref. [3] calculated with the Yukawa potential. The arrow indicates the position of the topmost atomic layer.

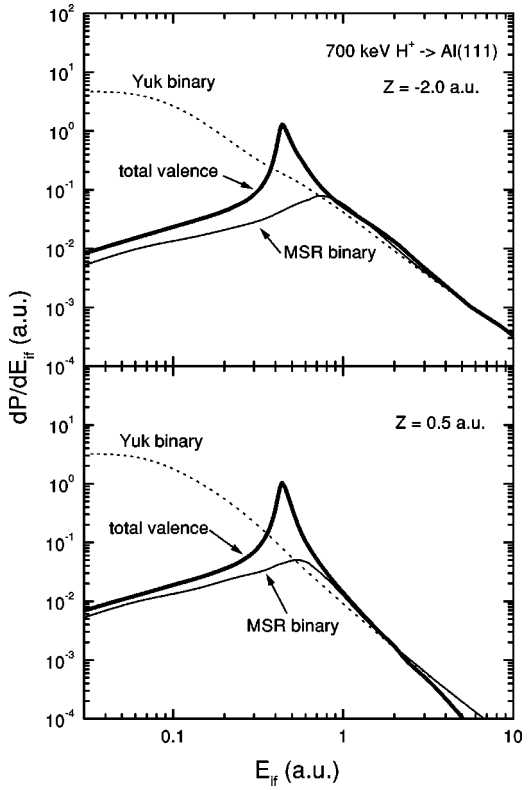

FIG. 3. Differential probability of energy loss, dP/dE_{if}, by collisions with the valence band, as a function of the lost energy E_{if}, for 700 keV protons impinging on an Al(111) surface. Two different projectile distances to the electronic surface are considered: $Z=-2$ and 0.5 a.u. Theories as in Fig. 2.

approximately ceded in equal parts to single-particle collisions and plasmon excitations. Instead, outside the electronic surface the MSR binary contribution rapidly tends to zero, and for large values of Z the difference between the total valence and binary energy losses is provided by the mechanism of excitation of surface plasmons.

Note that the energy-loss values obtained with the binary collisional formalism strongly depend on the model used to describe the screened P-e potential, as also observed in Ref. [4]. Whereas the MSR binary contribution runs below the total valence curve, the binary values obtained with the usual SR approximation, not shown here, overestimate the dielectric results in the proximity of the surface and in the vacuum region [4]. Thus, the validity of the usual SR model within the binary collisional formalism is questionable, at least near the surface.

To inspect in detail the behavior of the proposed model, in Fig. 3 we plot the differential probability of energy loss, dP/dE_{if}, as a function of the lost energy E_{if}. The values of dP/dE_{if} are derived from Eq. (8) taking into consideration that S can also be expressed as $S=\int dE_{if}E_{if}(dP/dE_{if})$. Two different distances to the electronic surface are considered: $Z=-2$ and 0.5 a.u. For both Z values, binary values calculated with the MSR model are lower than the total valence contribution, showing a smooth maximum at intermediate lost energies. The position of the binary maximum weakly depends on the projectile-surface distance and is related to the range of the wake potential [8]. Outside this energy region the binary curve approaches the dielectric one. The pronounced peak displayed by the total valence contribution at the surface plasmon frequency ω_s (shifted due to the plasmon dispersion) is caused by plasmon excitations. This mechanism of collective absorption of energy is not contained in the binary formalism, which essentially describes the interaction between two particles, the projectile and one active electron. Again, the energy-loss distribution corresponding to the mechanism of plasmon excitation can be reckoned as the difference between binary and dielectric contributions. No structure is present in the differential probability dP/dE_{if} obtained with the Yukawa potential, which overestimates the total valence distribution at low E_{if} values by more than two orders of magnitude. At high lost energies, instead, all the theories agree, indicating that they are describing head-on (Coulomb) collisions.

B. Electron emission probability

In this section we apply the MSR binary model to the calculation of electron emission from the free-electron gas. Since in Eq. (9) the electron momentum $\mathbf{k}_f$ is considered inside the solid, to compare our results with the experiments we change variables, $dP^3/d\mathbf{k}_f'=(\kappa_{fz}/k_{fz})dP^3/d\mathbf{k}_f$, where $\mathbf{k}_f'=(\mathbf{k}_{fs},\kappa_{fz})=k_f'(\cos\theta_e,0,\sin\theta_e)$ is the final electron mo-

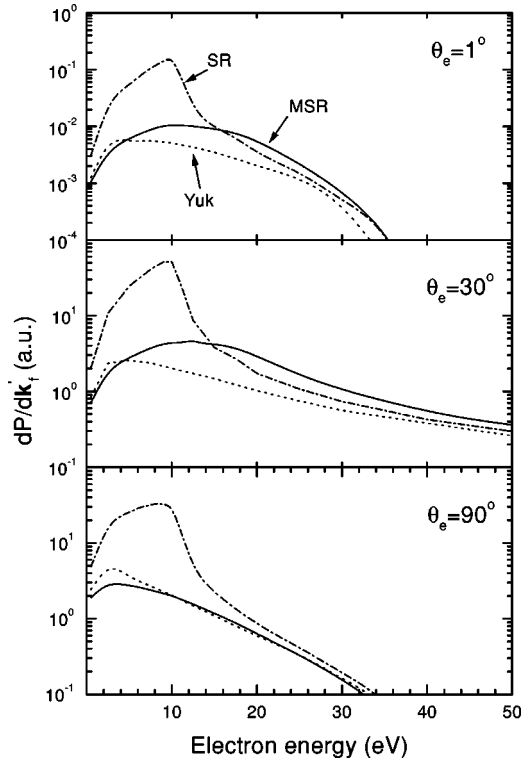

FIG. 4. Differential probability of electron emission from the valence band, $d^3P/d\mathbf{k}_f'$, for 100 keV protons impinging on an Al(111) surface with the incidence angle $\theta_i=1°$. Three ejection angles of the electron are considered: $\theta_e=1°$, 30°, and 90°. Solid and dash-dotted lines, binary emission probabilities calculated by using the MSR [Eq. (7)] and SR [Eq. (3)] models, respectively; dotted line, binary emission probability calculated with the Yukawa potential.

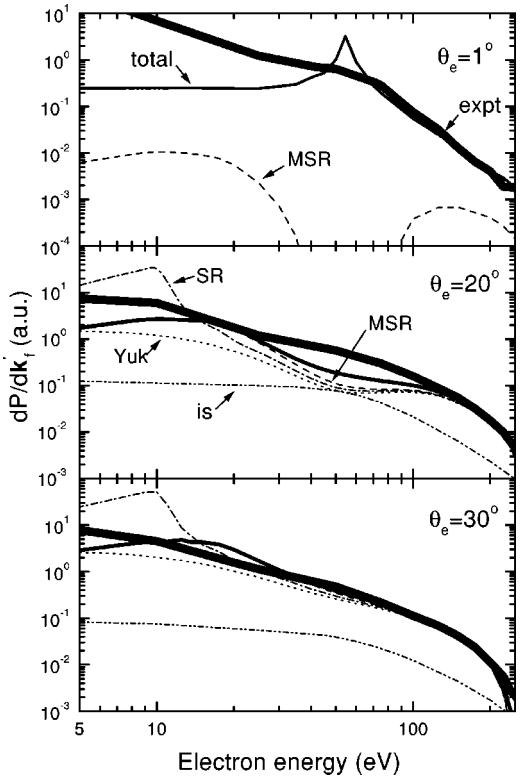

FIG. 5. Differential probability of electron emission for 100 keV protons impinging on an Al(111) surface with the incidence angle $\theta_i=1°$. Three electron emission angles are considered: $\theta_e=1°$, 20°, and 30°. Thin solid line, total probability of emission calculated by adding the binary valence (with the MSR model) and inner-shell contributions. Dashed, dash-dotted, and dotted lines, binary valence contributions evaluated by using the MSR, SR, and Yukawa potentials, respectively; dash–dot-dotted line, inner-shell contribution calculated with the CDW-EIS approximation. The thick solid line represents experimental data extracted from Ref. [11], normalized with our theoretical total values, as explained in the text.

mentum outside the solid, $\kappa_{fz}=(k_{fz}^2-k_c^2)^{1/2}$, and $k_c=(2V_0)^{1/2}$ [3]. Notice that the differential emission probability $dP^3/d\mathbf{k}_f'$ cannot be directly derived from the dielectric formalism. In Fig. 4 we plot $dP^3/d\mathbf{k}_f'$ as a function of the electron energy $\epsilon_{\mathbf{k}_f}=k_f'^2/2$ for 100 keV protons impinging on an Al(111) surface with the angle of incidence $\theta_i=1°$. Three different ejection angles of the electron, $\theta_e=1°$, 30°, and 90°, are considered. In the figure, binary results obtained with the MSR model [Eq. (7)] are compared with those calculated with the usual SR potential [Eq. (3)]. For the three ejection angles, all the binary theories coincide at high electron energy but differences arise as the electron energy decreases. At $\theta_e=1°$ and 30°, below 30 eV the MSR binary probability is higher than the one obtained with the Yukawa potential. This difference disappears as the ejection angle becomes close to the direction perpendicular to the surface plane, and at $\theta_e=90°$ the maximum of the MSR binary curve is slightly lower than that corresponding to the Yukawa potential. On the other hand, the binary results obtained with the usual SR model display a pronounced peak at electron energies around 10 eV for the three ejection angles. This peak is situated around the energy ω_s-E_F, shifted due to the plasmon dispersion, and its height strongly depends on the ejection angle. An equivalent peak was found by García de Abajo and Echenique [22] with a similar binary formalism. Certainly, this enhancement of the SR binary probability does *not* correspond to the plasmon decay mechanism. At low electron energies, a structure in the derivative spectrum is found experimentally [23,24,1,2], and it may be associated with plasmon decay [25]. But this process is not considered in the binary formalism, and in order to calculate it we need to develop a formulation that includes plasmon excitations as intermediate states [26].

With the aim of comparing the spectra of electron emission with experimental data [11] we add the contribution coming from the inner shells of the surface atoms to the binary valence emission. The inner-shell emission probability is calculated by employing a semiclassical formalism [12], in which the multiple collisions of the incident ion with the surface atoms are treated as single encounters with the outermost atoms along the projectile path. In the model the emission probability per unit path is expressed in terms of atomic probabilities, which are evaluated with the CDW-EIS approximation, taking into consideration the dependency not only on the modulus of the impact parameter but also on its direction.

The total emission probability obtained as the sum of valence and core contributions is plotted in Fig. 5, for 100 keV protons impinging on an Al(111) surface with the angle of incidence $\theta_i = 1°$. Under this condition of grazing incidence, transport effects are expected to play a minor role [27], at least for large ejection angles of the electron. In the calculation of the total probability, the binary emission from the valence band is evaluated with the MSR model. Again three ejection angles, $\theta_e = 1°$, 20°, and 30°, are considered. Total results are compared with the experimental data of Ref. [11], normalized by using our theoretical values for the electron energy of 200 eV. To distinguish angular and energy regions where each process is dominant, in Fig. 5 we also plot the partial contributions coming from valence and core electrons. Since the single-particle collisions with conduction electrons satisfy the energy conservation imposed by the δ function in Eq. (1), the values of $\mathbf{k}'_f$ corresponding to the binary mechanism are confined to the region $R_{\min} \leqslant |\mathbf{k}'_f - \mathbf{v}_{is}| \leqslant R_{\max}$, where $R_{\max} = [(v_{is}+v_F)^2 - k_c^2]^{1/2}$ and $R_{\min} = [(v_{is}-v_F)^2 - k_c^2]^{1/2}\Theta(v_{is}-(k_c+v_F))$. We observe that at the angle $\theta_e = 1°$ the inner-shell emission is one order of magnitude higher than the valence emission. For the lowest electron energies the footprint of the valence enhancement is completely erased from the total spectrum by the core contribution. In this electron energy region the large difference between theoretical and experimental values could be provided by other mechanisms, including multiple scattering processes [6]. At this particular emission angle, $\theta_e = 1°$, the probability of inner-shell ionization shows a peak that corresponds to the well-known capture to the continuum (CTC) peak, convoluted by the surface symmetry. There is no binary contribution from the valence band in the electron energy region around the CTC peak. However, as the ejection angle increases the binary emission from the valence band gives the more important contribution. Just for $\theta_e = 20°$ and 30°, we also show the partial contribution from the valence band evaluated with the usual SR binary theory. For both ejection angles, results obtained with the MSR model are in reasonable agreement with the experiments, while the pronounced peak displayed by the SR binary curve greatly overestimates the experimental data at low electron energies. Precisely at these energies the MSR model predicts a binary background quite different from that derived with the simple Yukawa potential. The knowledge of the binary valence emission is essential there to determine the contribution of the plasmon decay mechanism [2] to the emission spectrum.

IV. CONCLUSIONS

Within the binary collisional formalism we have developed a model to describe the effective P-e potential, which is based on the usual SR approximation. The proposed model, called the MSR model, incorporates the component of the transferred electron momentum perpendicular to the surface in the dispersion of the medium, thus correcting the unphysical peaks found in the SR binary theory [4]. The binary energy loss calculated with the MSR model runs below the total valence contribution, as expected. Inside the solid, the binary values satisfy the equipartition rule, which states that binary and collective energy losses are similar for high projectile velocities. In the vacuum region, instead, the contribution of single-particle collisions rapidly decreases, and only the mechanism of surface plasmon excitation survives.

The electron emission induced by the projectile is also studied with the MSR binary theory. Differential emission probabilities are compared with those obtained with the usual SR potential, and differences are found at low electron energies. With the aim of comparing the emission spectra with available experiments we also evaluate ionization from atomic inner shells with the CDW-EIS approximation. The total results calculated with the MSR model show reasonable agreement with experimental data for large ejection angles of the electron. On the contrary, the usual SR model gives a pronounced binary peak at low electron energies, whose existence is not experimentally supported. Although the measured electronic distributions present an enhancement around the surface plasmon frequency, it is much lower than the one provided by the SR model, and this experimental structure is not a product of binary collisions as calculated here, but a consequence of the decay of the surface plasmon after interacting with a single electron. The present results are thus important to calculate more precisely the binary background in the plasmon decay region of the energy spectrum.

[1] S.M. Ritzau, R.A. Baragiola, and R.C. Monreal, Phys. Rev. B **59**, 15 506 (1999).

[2] E.A. Sánchez, J.E. Gayone, M.L. Martiarena, O. Grizzi, and R.A. Baragiola, Phys. Rev. B **61**, 14 209 (2000).

[3] M.S. Gravielle, Phys. Rev. A **58**, 4622 (1998).

[4] M.S. Gravielle, D.G. Arbó, and J.E. Miraglia, Nucl. Instrum. Methods Phys. Res. B **182**, 29 (2001).

[5] J. Burgdörfer, in *Progress in Atomic and Molecular Physics*, edited by C. D. Lin (World Scientific, Singapore, 1993).

[6] C.O. Reinhold and J. Burgdörfer, Phys. Rev. A **55**, 450 (1997).

[7] R.H. Ritchie and A.L. Marusak, Surf. Sci. **4**, 234 (1966).

[8] F.J. García de Abajo and P.M. Echenique, Phys. Rev. B **46**, 2663 (1992); **48**, 13 399 (1993).

[9] J.I. Juaristi, F.J. García de Abajo, and P.M. Echenique, Phys. Rev. B **53**, 13 839 (1996).

[10] Y. Wang and W.K. Liu, Phys. Rev. A **54**, 636 (1996).

[11] M.L. Martiarena, E.A. Sánchez, O. Grizzi, and V.H. Ponce, Phys. Rev. A **53**, 895 (1996).

[12] M.S. Gravielle, Phys. Rev. A **62**, 062903 (2000).

[13] H. Winter, R. Kirsch, J.C. Poizat, and J. Remillieux, Phys. Rev. A **43**, 1660 (1991).

[14] J.E. Miraglia, Phys. Rev. A **50**, 2410 (1994); M.S. Gravielle and J.E. Miraglia, *ibid.* **50**, 2425 (1994); **50**, 3202 (1994).

[15] D.G. Arbó and J.E. Miraglia, Phys. Rev. A **58**, 2970 (1998).

[16] V.G. Molière, Z. Naturforsch. A **2**, 133 (1947).

[17] N.R. Arista, Phys. Rev. A **49**, 1885 (1994).

[18] J. Lindhard and A. Winther, Mat. Fys. Medd. K. Dan. Vidensk. Selsk. **34**, 4 (1964).
[19] N.D. Mermin, Phys. Rev. B **1**, 2362 (1970).
[20] I. Nagy and P.M. Echenique, Phys. Rev. A **47**, 3050 (1993); I. Nagy and B. Apagyi, *ibid.* **58**, R1653 (1998).
[21] H. Winter, H. Wilke, and M. Bergomaz, Nucl. Instrum. Methods Phys. Res. B **125**, 124 (1997).
[22] F.J. García de Abajo and P.M. Echenique, Nucl. Instrum. Methods Phys. Res. B **79**, 15 (1993); F.J. García de Abajo, *ibid.* **98**, 445 (1995).
[23] C. Benazeth, N. Benazeth, and L. Viel, Surf. Sci. **78**, 62 (1978).
[24] D. Hasselkamp and A. Scharmann, Surf. Sci. **119**, L38 (1982).
[25] D.L. Mills, Surf. Sci. **294**, 161 (1993).
[26] M. Rösler, Appl. Phys. A: Mater. Sci. Process. **61**, 595 (1995); Scanning Microsc. **10**, 1025 (1996).
[27] K. Kimura, S. Ooki, G. Andou, K. Nakajima, and M. Mannami, Phys. Rev. A **58**, 1282 (1998).